TRAMP-mediated RNA surveillance prevents spurious entry of RNAs into the *Schizosaccharomyces pombe* siRNA pathway

Marc Bühler[1,3,4], Noah Spies[2,4], David P Bartel[2] & Danesh Moazed[1]

In the fission yeast *Schizosaccharomyces pombe*, the RNA interference (RNAi) machinery is required to generate small interfering RNAs (siRNAs) that mediate heterochromatic gene silencing. Efficient silencing also requires the TRAMP complex, which contains the noncanonical Cid14 poly(A) polymerase and targets aberrant RNAs for degradation. Here we use high-throughput sequencing to analyze Argonaute-associated small RNAs (sRNAs) in both the presence and absence of Cid14. Most sRNAs in fission yeast start with a 5′ uracil, and we argue these are loaded most efficiently into Argonaute. In wild-type cells most sRNAs match to repeated regions of the genome, whereas in *cid14Δ* cells the sRNA profile changes to include major new classes of sRNAs originating from ribosomal RNAs and a tRNA. Thus, Cid14 prevents certain abundant RNAs from becoming substrates for the RNAi machinery, thereby freeing the RNAi machinery to act on its proper targets.

RNAi is a conserved silencing mechanism that is triggered by double-stranded RNA (dsRNA)[1,2]. Silencing is mediated by small interfering RNAs (siRNAs) of about 22 nucleotides (nt) in size, which are produced from the long dsRNA by the Dicer RNase[3–7]. siRNAs guide Argonaute proteins to complementary nucleic acids where they promote the inactivation of the homologous sequences. In some systems, efficient RNAi requires synthesis of dsRNA by an RNA-directed RNA polymerase (RdRP)[8,9]. Besides their role in post-transcriptional gene silencing (PTGS), siRNAs have also been implicated in regulation at the DNA and chromatin levels in plants and some fungi[10,11].

The role of siRNAs in gene regulation at the chromatin level has been well studied in fission yeast, whose genome encodes a single gene each for Argonaute, Dicer and RdRP: *ago1+*, *dcr1+* and *rdp1+*, respectively. At centromeres, deletion of any of these genes results in a loss of gene silencing, reduced histone H3 lysine 9 (H3K9) methylation and Swi6 (the homolog of heterochromatin protein-1 (HP1)) localization, all of which are conserved molecular markers of heterochromatin[12]. Ago1 is found in the RNA-induced transcriptional silencing (RITS) and Argonaute siRNA chaperone (ARC) complexes[13,14]. Early sequencing of small RNAs from fission yeast revealed heterochromatic siRNAs that match centromeric repeats[15]. In addition, ∼1,300 siRNAs isolated from the RITS complex, using a tag on its Chp1 subunit, have been reported[16]. These RITS-associated siRNAs are 20–22-nt long and map to repeat elements embedded in heterochromatic regions, the ribosomal DNA (rDNA) array, intergenic regions, mRNAs, tRNAs, subtelomeric and silent mating-type regions[16]. Generation of these siRNAs requires Dicer, Argonaute and Rdp1 (refs. 13,17,18).

The RNAi pathway is essential for high levels of H3K9 methylation and gene silencing at fission yeast centromeres, but it is dispensable at other heterochromatic loci such as telomeres or the silent mating-type loci[12,19]. Although heterochromatin has long been thought to be transcriptionally inactive, recent observations in fission yeast show that heterochromatic domains are transcribed to some degree[12,18,20,21]. However, the resulting heterochromatic transcripts are rapidly turned over by a mechanism called co-transcriptional gene silencing (CTGS)[11,18]. Although possibly mediated by the RNAi pathway at centromeres, CTGS at other fission yeast heterochromatic regions depends on a specialized polyadenylation complex referred to as the TRAMP (Trf4-Air1/Air2-Mtr4 polyadenylation) complex[22], most likely targeting heterochromatic transcripts for degradation by the exosome[20].

The role of TRAMP in exosome-mediated degradation of aberrant RNAs was first described in budding yeast[22]. Homologs of the budding yeast TRAMP subunits Trf4/5, Air1/2 and Mtr4 are found in the fission yeast TRAMP complex[20]. The *S. pombe* homolog of the budding yeast Trf4/5 poly(A) polymerases is Cid14, a member of the Cid1 family of noncanonical poly(A) polymerases[23]. Cid14 is required for polyadenylation of ribosomal RNAs (rRNAs) and proper chromosome segregation[24]. In addition to its role in rRNA biogenesis and CTGS, deletion of *cid14+* results in a dramatic decrease in

[1]Department of Cell Biology, 240 Longwood Avenue, Harvard Medical School, Boston, Massachusetts 02115 USA. [2]Howard Hughes Medical Institute and Department of Biology, Massachusetts Institute of Technology and Whitehead Institute for Biomedical Research, 9 Cambridge Center, Cambridge, Massachusetts 02142, USA. [3]Present address: Friedrich Miescher Institute for Biomedical Research, Maulbeerstrasse 66, 4058 Basel, Switzerland. [4]These authors contributed equally to this work. Correspondence should be addressed to D.P.B. (dbartel@wi.mit.edu) or D.M. (danesh@hms.harvard.edu).
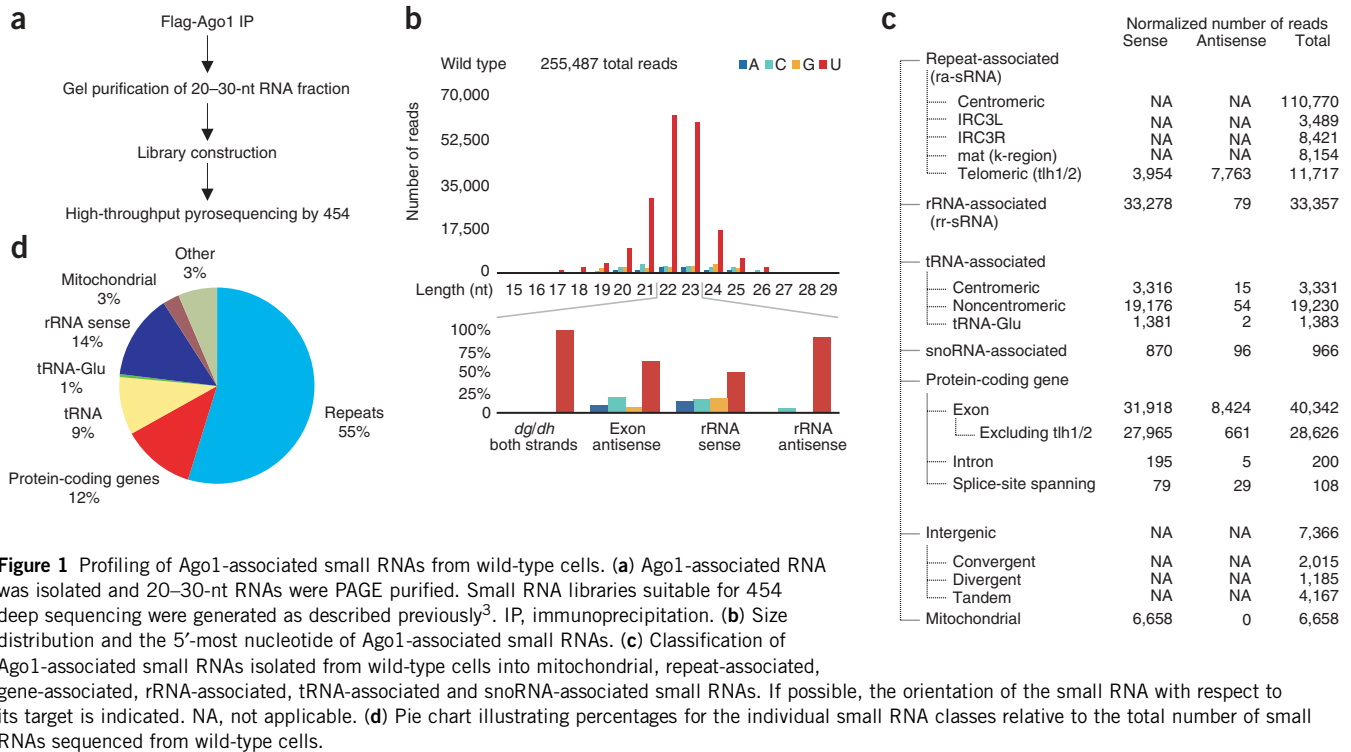
Figure 1 Profiling of Ago1-associated small RNAs from wild-type cells. (**a**) Ago1-associated RNA was isolated and 20–30-nt RNAs were PAGE purified. Small RNA libraries suitable for 454 deep sequencing were generated as described previously[3]. IP, immunoprecipitation. (**b**) Size distribution and the 5′-most nucleotide of Ago1-associated small RNAs. (**c**) Classification of Ago1-associated small RNAs isolated from wild-type cells into mitochondrial, repeat-associated, gene-associated, rRNA-associated, tRNA-associated and snoRNA-associated small RNAs. If possible, the orientation of the small RNA with respect to its target is indicated. NA, not applicable. (**d**) Pie chart illustrating percentages for the individual small RNA classes relative to the total number of small RNAs sequenced from wild-type cells.

centromeric siRNA levels, suggesting a role for Cid14 in siRNA biogenesis or stabilization[20].

To better understand the role of Cid14 in accumulation of centromeric siRNAs, we used high-throughput sequencing to examine Ago1-associated small RNAs in wild-type and *cid14Δ* fission yeast cells. Most of the small RNAs recovered by an Ago1 pull-down start with a 5′ U and are 22 nt or 23 nt long. In wild-type cells, most Ago1-associated small RNAs correspond to repetitive DNA elements found at the centromeres. Other Ago1-associated small RNAs match the sequences of tRNAs, small nucleolar RNAs (snoRNAs), rDNA and intergenic regions. The small RNA profile changes dramatically in *cid14Δ* cells. Consistent with previous findings[20], the levels of centromeric siRNAs are reduced in *cid14Δ* cells, whereas the levels of other small RNAs increase dramatically. The most prominent new class of small RNAs in *cid14Δ* cells includes those that match tRNA-Glu and ribosomal RNA sequences, which are normally substrates of TRAMP[22,24–26]. These findings indicate that Cid14 acts as a negative regulator of siRNA biogenesis by competing with the RNAi machinery for substrates.

RESULTS

Ago1-associated small RNAs

To obtain a more comprehensive view of the *S. pombe* siRNA profile and to better understand the connection between Cid14 and RNAi[20], we generated small RNA libraries from affinity-purified Flag-tagged Ago1. These libraries should contain siRNAs from RITS, ARC and free or other possible Ago1 complexes. We then subjected the libraries to high-throughput pyrosequencing[27] (**Fig. 1a**). Analysis of ∼200,000 sequences showed that most of the Ago1-associated small RNAs derived from wild-type cells were 22 nt or 23 nt long (**Fig. 1b**) and that most matched repetitive elements in the genome (55%, **Fig. 1c,d**). Other small RNAs matched annotated sequences of rDNA, tRNAs, snoRNAs, intergenic regions, introns, exons and mitochondrial DNA

(**Fig. 1c,d**). We classified Ago1-associated small RNAs as siRNAs and sRNAs. The term 'siRNA' was used when there was evidence that Dcr1 generated the small RNA. In other cases, Ago1 seemed to be associated with small RNAs that corresponded to abundant cellular RNAs and derived from mostly the sense strand, and thus seemed to be generated primarily by non-Dcr1 degradation processes. For example, no reads were antisense to mitochondrial genes, suggesting that all mitochondrial reads were fragments of normal transcripts. To distinguish this set of small RNAs, we refer to them throughout this work as 'sRNAs'. Although some sRNAs, such as antisense gene-specific sRNAs, might be produced by Dcr1 and could have physiological roles, a larger fraction seemed to be degradation products that may nonspecifically associate with overexpressed Flag-Ago1. In this paper, we focus on the small RNA populations that either derived from centromeric repeat sequences or showed a shift in their abundance in *cid14Δ* cells.

General properties of Ago1-associated siRNAs

Consistent with previous reports[16,20], siRNAs corresponding to the centromeric *dg* and *dh* repeats were present in the Ago-associated small RNA pool, with similar numbers matching the forward and reverse strands. Most siRNAs in plants also derive from both DNA strands[28], whereas those in *Caenorhabditis elegans* are predominantly antisense to mRNAs[29,30]. In *S. pombe*, the origin from both strands probably reflects RNA polymerase II (RNA Pol II) transcription in both directions, which gives rise to forward and reverse transcripts that are then converted to dsRNA by the RNA-directed RNA polymerase complex (RDRC).

As observed for some classes of Argonaute-associated sRNAs in other lineages[30–38], a large majority (>98%) of the siRNAs corresponding to centromeric *dg* and *dh* repeats started with a 5′ U (**Fig. 1b**). Previous projects using the same methods for library construction and sequencing revealed classes of siRNAs that started predominantly with 5′ guanosine and another that started mostly with

Table 1 5′ nucleotide preference for centromeric reads

Informative inferred duplexes

Comparison	Preference	Duplexes compared		Reads
U vs. G	99.9%	5′ U...................C.. 3′		7,423
		3′ ..A...................G 5′		4
U vs. C	99.7%	5′ U...................G.. 3′		7,835
		3′ ..A...................C 5′		24
U vs. A	99%	5′ U...................U.. 3′		9,245
		3′ ..A...................A 5′		90
A vs. G.	96%	5′ A...................C.. 3′		123
		3′ ..U...................G 5′		4
A vs. C	78%	5′ A...................G.. 3′		88
		3′ ..U...................C 5′		23
G vs. C	0%	5′ G...................G.. 3′		0
		3′ ..C...................C 5′		7

Other inferred duplexes

Comparison		Duplexes compared		Reads
A vs. A		5′ A...................U.. 3′		99
		3′ ..U...................A 5′		
C vs. C		5′ C...................G.. 3′		15
		3′ ..G...................C 5′		
G vs. G		5′ G...................C.. 3′		0
		3′ ..C...................G 5′		
U vs. U		5′ U...................A.. 3′		7,654
		3′ ..A...................U 5′		

For the informative duplexes, each comparison indicates the number of 23-nt centromeric reads with the given nucleotides at positions 1 and 21 relative to the total number of reads from either strand of the inferred duplex. For any given read, we did not require a read from the opposite strand. For example, we found 7,423 reads with a 5′ U and a C at position 21, but only 4 reads with 5′ G and A at position 21. We assumed that every read with a C at position 21 was once part of a duplex with an opposite strand whose 5′ nucleotide was G, and hence calculated the U versus G preference as 7,423 / (7,423 + 4)*100%=99.9%. Similar preferences were obtained when we required reads from both strands for every duplex, although some duplexes were not present at all in the centromeric reads. Also listed are reads from the other four types of inferred duplexes, which were not informative for assessing strand preferences.

5′ adenosine, thereby indicating that our method does not artifactually favor the sequencing of RNAs with 5′ U[28,30]. Processing of the double-stranded RNA was also unlikely to explain most of this extreme bias for RNAs with 5′ U, because Dicer cleavage is thought to occur sequentially in 22–23-nt intervals, and the genome does not encode uracil at such regularly spaced intervals. Nonetheless, processing preferences could contribute to this bias, and we uncovered some evidence that they do contribute to a small degree.

Because the siRNAs were predominantly a near-equal mixture of 22-mers and 23-mers, a reasonable proposal would be that Dicer has some leeway in choosing the precise cleavage site and that sequence context might influence the choice of whether to cleave to produce 22-nt siRNAs or to cleave at the next base pair to produce 23-nt siRNAs. Therefore, we examined all 16 dinucleotide possibilities at positions 23 and 24, counting from the 5′ end of each sequenced siRNA (Supplementary Table 1 online). As would be expected if Dicer prefers to cleave before a uracil and thereby preferentially generates a downstream siRNA beginning with uracil, we observed a propensity toward 22-mers when the nucleotide at position 23 was a uracil. Other notable biases suggested that Dicer prefers to cleave at sites that avoid creating an siRNA beginning with G. However, all of these propensities were modest, generally less than three-fold, indicating that preferential

siRNA processing contributes relatively little to the striking preference for 5′ U. Having ruled out a more-than-modest effect of preferential processing, we conclude that preferential stability of siRNAs beginning with U explains most of the bias for a 5′ U. This preferential stability could be at different levels, including preferential stability before encountering Ago1 or preferential stability after loading into Ago1. A reasonable hypothesis is that the much higher stability of 5′ U siRNAs arises primarily from a strong preference of Ago1 for loading siRNAs beginning with a 5′ U, and that those siRNAs that Ago1 rejects because they do not begin with a U are rapidly degraded.

To investigate 5′ nucleotide preferences in more depth, we considered the inferred siRNA duplexes corresponding to sequenced 23-mers deriving from the centromeric *dg/dh* repeats. (The choice of 23-mers over 22-mers stemmed from the notion that these longer siRNAs were less likely to be degradation intermediates of longer siRNAs.) When considering the influence of the 5′ nucleotide on siRNA loading and stability, six classes of duplexes that each involved siRNAs with different 5′ nucleotides were informative (Table 1). Regardless of the duplex under consideration, a consistent hierarchy was observed in the sequenced reads, with 5′ U >> A > C > G.

The >100-fold bias in reads from the strand beginning with a 5′ U was consistent with the idea that one of the two siRNA strands, the passenger strand, was discarded during loading[14,39,40], probably after cleavage of the passenger strand by the inherent slicer activity of Ago1 (refs. 14,41). Moreover, this bias showed that nearly all of the siRNAs that were sequenced were already single stranded, which indicated that in fission yeast the siRNA duplex is transient when compared to the loaded single strand. Furthermore, the predicted pairing asymmetry[42] had no correlation with the most frequently sequenced strand of these duplexes (Supplementary Table 2 and Supplementary Results online), as has been reported for endogenous siRNAs of plants[28].

Having ruled out pairing asymmetry as a factor influencing strand choice, we examined whether strand choice might be influenced by the identity of the 5′ nucleotide. As mentioned earlier, one hypothesis for explaining the abundance of siRNAs beginning with U is that Ago1 has a strong preference for loading siRNAs beginning with a 5′ U, and that those siRNAs that Ago1 rejects because they do not begin with a U are rapidly degraded. The alternative hypothesis is that siRNAs are loaded equally efficiently regardless of their 5′ nucleotide, and those siRNAs beginning with G, C and A are much less stable after loading than those are those beginning with U. Examination of the reads matching centromeric *dg/dh* repeats indicated that 5′ U siRNAs were more likely to be associated with Ago1 if they were paired originally to a 5′ A siRNA than if they were paired with another 5′ U siRNA. Because the model positing differential post-loading stabilities cannot explain this observation, but the model positing differential loading can explain it, we conclude that at least part of the 5′ U bias is due to the preferential loading of siRNAs beginning with U (Supplementary Results and Supplementary Fig. 1 online).

The cells used for the isolation of Ago1-associated small RNAs in our experiments contained a *ura4*+ transgene inserted into the outer centromeric repeats on the right arm of chromosome 1 (*otr1R ::ura4*+)[43]. We sequenced 249 siRNAs (20–25 nt) that corresponded to *ura4*+ sequences (Fig. 2a and Supplementary Table 3 online). Like the cen siRNAs, *ura4*+ siRNAs showed a preference for uracil at their 5′ terminus, but, unlike the cen siRNAs and consistent with previous results[20], *ura4*+ siRNAs showed a five-fold preference for the sense strand (206 sense, 43 antisense; Fig. 2a–c and Supplementary Table 3).

More than 90% of the antisense reads corresponding to coding exons matched *tlh1* and *tlh2* (Fig. 1c), which are subtelomeric genes classified as 'repeat associated'. The remaining 661 reads antisense to
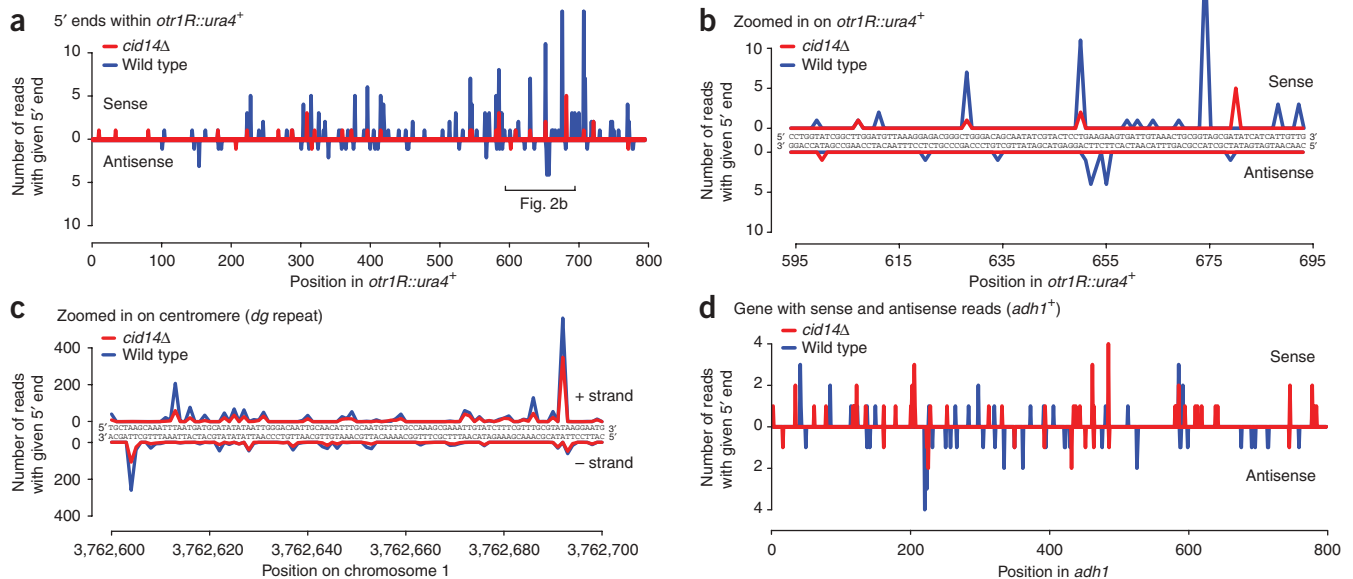
Figure 2 Distribution of reads mapping to genomic loci. (**a**) Distribution of siRNAs at a *ura4*[+] transgene inserted into the outermost centromeric repeats on the right arm of chromosome 1 (*otr1R ::ura4*[+]). *ura4*[+] small RNAs show a five-fold preference for the sense strand, and only one of the two strands is found in Ago1. Peaks indicate the number of *ura4*[+] reads with 5′ ends at each genomic position. (**b**) Zoomed in version of **a**. Note that nearly all of the reads start with a T (U). (**c**) Distribution of siRNAs at a centromeric *dg* repeat. For any given position, generally only one of the two centromeric siRNA strands, starting with a T (U), is present in Ago1. (**d**) Distribution of sRNAs at the endogenous *adh1*[+] gene.

protein-coding exons were distributed among 341 genes, usually in far lower numbers than those of sense reads, although for *adh1*[+] the numbers were roughly equal (**Fig. 2d** and **Supplementary Table 3**).

Small RNA profile changes in *cid14Δ* cells

In addition to its role in rRNA biogenesis and CTGS, Cid14 has been proposed to be involved in siRNA generation, as deletion of *cid14*[+] results in a dramatic decrease in centromeric repeat-associated siRNA levels[20]. We found that deletion of *cid14*[+] had no effect on the size distribution of siRNAs (**Fig. 3**). Consistent with previous findings, we observed a marked (five-fold) decrease in the fraction of reads mapping to centromeric repeats in *cid14Δ* cells (compare **Fig. 1c,d** with **Fig. 3a,c**). However, other classes of Ago1-associated small RNAs spanning many regions across all three chromosomes increased disproportionately (**Fig. 3d**), the most prominent among them being small RNAs antisense to rRNA, which increased by 274-fold (compare **Fig. 1c** with **Fig. 3a,c**). Both rRNAs and tRNAs have previously been shown to be targets for processing or degradation by the TRAMP and exosome pathway[22,24–26]. In contrast, the fraction of reads from gene-specific sense and antisense sRNAs were similar in wild-type and *cid14Δ* cells (increases of 1.4-fold and 1.1-fold, respectively). Our observations suggest that, in cells lacking Cid14, accumulated rRNAs become substrates for the RNAi pathway and give rise to siRNAs.

Internal repeat elements flank the centromeric repeat regions of chromosome 3 (Internal repeat centromere 3, IRC3R, **Fig. 4a**) and coincide precisely with a sharp decrease in H3K9 methylation and Swi6 levels[16]. Therefore, they have been proposed to serve as boundary elements, similar to tRNA genes[44], that prohibit spreading of heterochromatin to euchromatic regions surrounding centromeres. H3K9 methylation levels at fission yeast centromeres, including *dg/dh* repeats and IRC elements[16], are reduced substantially in cells lacking siRNAs (*dcr1Δ*), and RNAi has an essential role in the proper assembly of heterochromatin at these repeat elements. Consistent with previous results, in *cid14Δ* cells, centromeric siRNA levels were reduced by

about 20-fold, but the levels of H3K9 methylation at the centromeric *dg/dh* repeats were unaffected[20] (**Fig. 3** and **Fig. 4b**). This reduction was far greater at IRC sequences, where we observed a nearly complete loss of siRNAs in *cid14Δ* cells (**Fig. 4a**).

To determine the possible contribution of RNAi, heterochromatin and the TRAMP and exosome pathways to the regulation of IRC transcripts, we used quantitative reverse-transcription PCR (RT-PCR) to analyze IRC3R transcript levels in cells that carried deletions or mutations in an essential gene in each pathway. IRC3R transcript levels were unaffected in *clr4Δ* and *dcr1Δ* cells (**Fig. 4c**), suggesting that these transcripts were not silenced by RNAi-mediated heterochromatin formation. In contrast, IRC3R transcript levels increased five- to seven-fold in *cid14Δ*, *mtr4-1* and *dis3-54* mutant cells, indicating that IRC3R is a substrate of the TRAMP (Cid14/Mtr4) and the exosome (Dis3) pathways (**Fig. 4c**). Furthermore, deletion of *rrp6*[+], a subunit of the nuclear exosome, did not affect IRC3R transcript levels, suggesting that degradation occurs in the cytoplasm rather than in the nucleus. We next asked whether H3K9me levels at the IRC on the right arm of chromosome 3 (IRC3R) were affected in *cid14Δ* cells. Unexpectedly, we did not detect any difference in H3K9 methylation levels between wild-type and *cid14Δ* cells (**Fig. 4b**). In contrast, H3K9 methylation has been shown to be absent at IRCs in *dcr1Δ* cells[16]. Together, these observations suggest that the spreading of H3K9 methylation into the IRC regions can occur independently of siRNAs but may be lost in *dcr1Δ* cells because of defects in RNAi-mediated nucleation of heterochromatin at the *dg/dh* repeats.

The sRNAs corresponding to the 5′ end of tRNA-Glu formed the third largest class of small RNAs found in the *cid14Δ* library (**Fig. 3c**). Whereas these RNAs were sequenced 1,381 times in wild-type cells, they were sequenced 30,850 times in *cid14Δ* cells (**Fig. 3a,c** and **Fig. 4d**). They also were clearly much more abundant than any other sRNAs mapping to tRNAs. Consistent with the sequencing data, the tRNA-Glu sRNA was specifically detected on northern blots of Ago1-associated RNAs from *cid14Δ* cells, but not from

wild-type cells (**Fig. 4e**). The larger tRNA fragments present in Flag-Ago1 preparations were background RNAs, because they were also recovered from an untagged Ago1 strain (**Fig. 4f**). In contrast, tRNA-Glu sRNA was present only in Flag-Ago1 pull-downs (**Fig. 4f**). However, the tRNA-Glu sRNA was not generated by Dcr1 or Rdp1 (**Fig. 4e**). This observation is consistent with the idea that abundant small RNAs, which are in the size range of siRNAs, can associate with Ago1. However, the physiological significance of this association remains to be determined. In particular, chromatin immunoprecipitation (ChIP) experiments indicated that there was no increase in histone H3K9 methylation at the tRNA-Glu locus in *cid14Δ* cells (**Fig. 4g**). Sense sRNAs loaded onto Ago1 may be unable to initiate H3K9 methylation because they cannot base pair with sense nascent tRNA-Glu transcripts. The propensity of this sRNA to associate with Ago1 might stem in part from its 5′ U, although 10 of the other 69 unique tRNAs also begin with U.

Ribosomal RNAs give rise to antisense siRNAs in *cid14Δ* cells
Small RNAs mapping to rDNA were identified previously and represented about 30% of the total number of sequences in the collection of ~1,300 RITS-associated small RNAs[16]. However, fragments of the abundant rRNAs are present in nearly all small RNA sequence libraries, and it had remained unclear whether these rRNA-associated small RNAs were produced by the RNAi pathway or were degradation products. We observed that in wild-type cells small RNAs corresponding to rRNAs were mainly of the sense orientation (**Fig. 5a,b**), and furthermore, were generated independently of the RNAi pathway (**Fig. 5c**), suggesting that they may be rRNA degradation products that nonspecifically associate with Ago1. In *cid14Δ* cells, we observed a dramatic increase in small RNAs of the opposite orientation (antisense). Unlike the sense-strand small RNAs, antisense ribosomal small RNAs required Rdp1 and Dcr1 for their biogenesis (**Fig. 5c**). These antisense ribosomal small RNAs were therefore classified with confidence as siRNAs (rr-siRNA). Ribosomal RNA genes are transcribed as a unit by RNA polymerase I, and the completed transcript is rapidly processed to form the mature 18S, 5.8S and 28S rRNAs[45] (**Fig. 5a**). Notably, antisense rr-siRNAs were more or less equally distributed along the 18S and 5.8S rRNAs, whereas most of the antisense 28S rr-siRNAs mapped to the 3′ end (**Fig. 5b**). Together, these observations suggested that, in *cid14Δ* cells, rRNAs become substrates for dsRNA synthesis by the RDRC complex and processing into siRNAs by Dcr1, thereby suggesting competition between the components of the RNAi machinery and possible degradation or processing initiated by the TRAMP complex. The RNAi pathway is required for H3K9 methylation and silencing of foreign promoters inserted within the rDNA repeats[16], suggesting that the low levels of rr-siRNAs observed in *cid14+* cells are functional. The dramatic increase in rr-siRNA levels in *cid14Δ* cells is likely to increase the efficiency of rDNA silencing and rDNA H3K9 methylation. Our efforts to unambiguously determine the role of Cid14 in regulation of rDNA H3K9 methylation were unsuccessful, probably because of the previously described variations in rDNA copy number in *cid14Δ* cells[46].
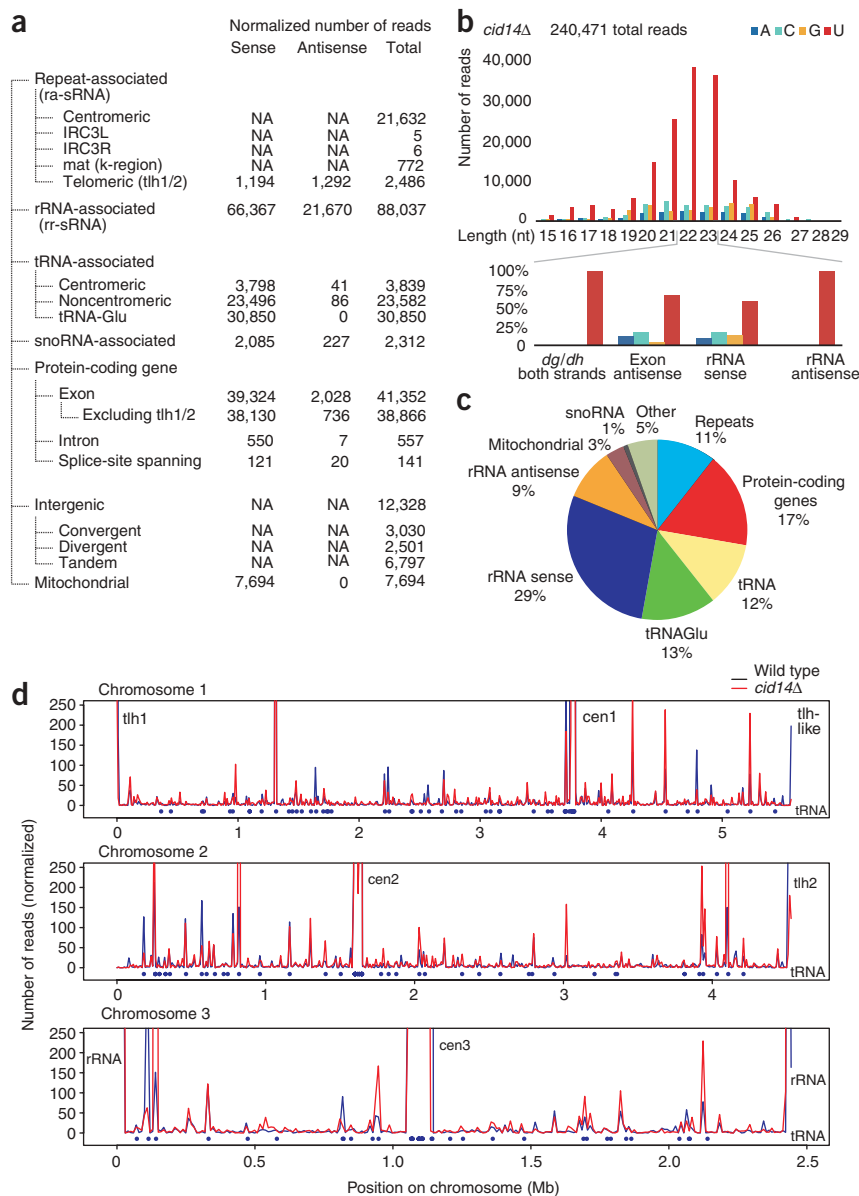
Deletion of Clr4 gives rise to antisense rr-siRNAs
In addition to components of the RNAi pathway, the Clr4 H3K9 methyltransferase and its associated factors are required for centromeric
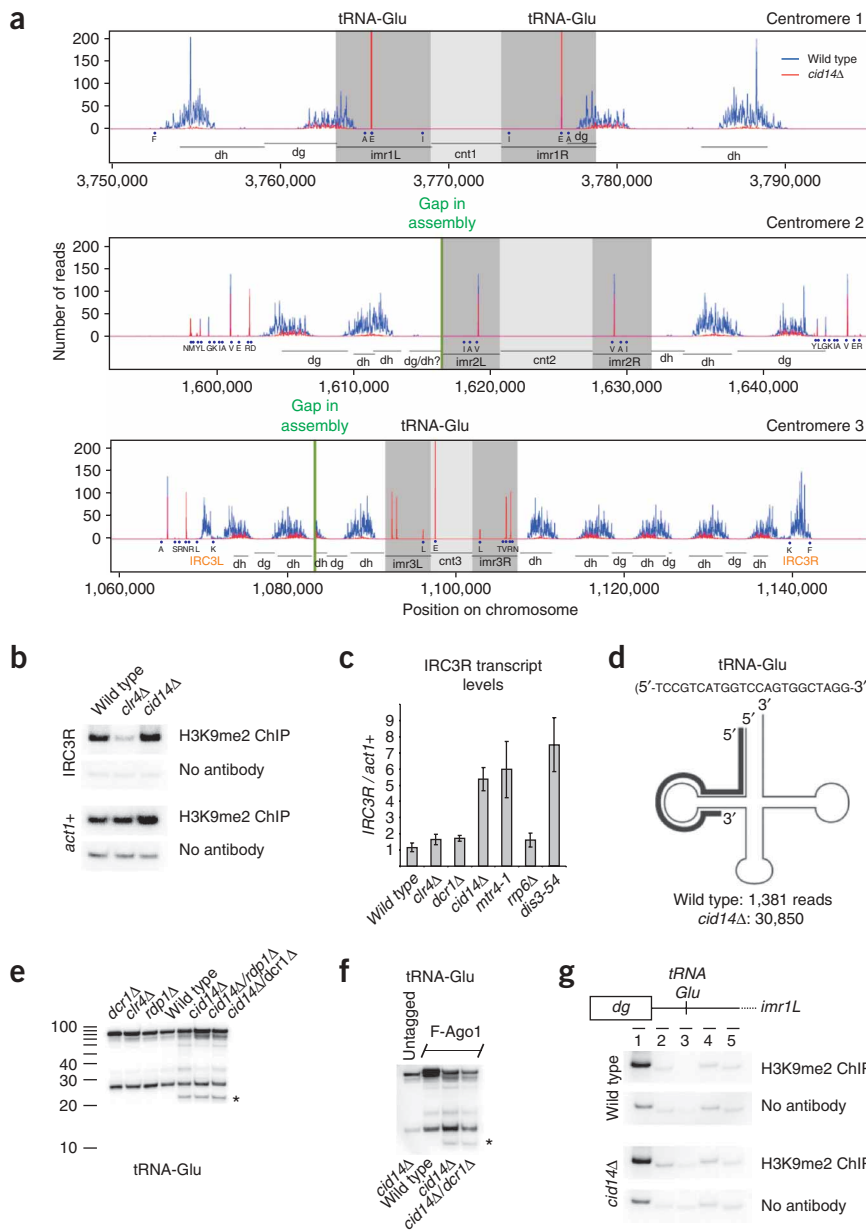

a

	Normalized number of reads		
	Sense	Antisense	Total
Repeat-associated (ra-sRNA)			
Centromeric	NA	NA	21,632
IRC3L	NA	NA	5
IRC3R	NA	NA	6
mat (k-region)	NA	NA	772
Telomeric (tlh1/2)	1,194	1,292	2,486
rRNA-associated (rr-sRNA)	66,367	21,670	88,037
tRNA-associated			
Centromeric	3,798	41	3,839
Noncentromeric	23,496	86	23,582
tRNA-Glu	30,850	0	30,850
snoRNA-associated	2,085	227	2,312
Protein-coding gene			
Exon	39,324	2,028	41,352
Excluding tlh1/2	38,130	736	38,866
Intron	550	7	557
Splice-site spanning	121	20	141
Intergenic	NA	NA	12,328
Convergent	NA	NA	3,030
Divergent	NA	NA	2,501
Tandem	NA	NA	6,797
Mitochondrial	7,694	0	7,694

Figure 3 Profiling of Ago1-associated small RNAs from *cid14Δ* cells. Small RNA libraries suitable for 454 deep sequencing were generated as for wild-type cells. (**a**) Classification of Ago1-associated small RNAs isolated from *cid14Δ* cells into the same classes as shown in **Figure 1**. (**b**) Size distribution and indication of the 5′-most nucleotide of small RNAs. (**c**) Pie chart illustrating percentages for the individual small RNA classes relative to the total amount of small RNAs sequenced from *cid14Δ* cells. (**d**) Chromosomal distribution profiles of Ago1-associated small RNAs isolated from wild-type (blue) and *cid14Δ* (red) cells. Blue bullets indicate the location of tRNA genes.

Figure 4 Small RNAs generated from centromeres in wild-type and *cid14Δ* cells. (**a**) siRNA distribution at centromeres in wild-type (blue) and *cid14Δ* (red) cells. IRC3-L/R, unique inverted repeats flanking both the left and right sides of centromere 3 (ref. 9); blue bullets, tRNA genes in single letter amino acid code. Three identical tRNA-Glu genes are found in centromeric heterochromatin, as well as three noncentromeric genes with identical sequence. Because all reads come from regions of perfect identity, it is ambiguous from which tRNA-Glu locus or loci these reads originate. (**b**) Quantitative RT-PCR was performed to determine IRC transcript levels in various mutant backgrounds as indicated on the *x*-axes. H3K9me2, dimethylated H3K9. (**c**) ChIP experiment showing that H3K9me2 in *cid14Δ* cells, where siRNAs are absent, is not affected at IRC3R. DNA from ChIP reactions with or without an antibody against H3K9me2 was used for PCR with primers to amplify the indicated sequences. Error bars are s.d. (**d**) Cloverleaf schematic of tRNA-Glu. Bold line represents the most prevalent Ago1-associated small RNA (5′-TCCGTCATGGTCCAGTGGCTAGG-3′), which matches the tRNA-Glu 5′ end and D-loop. (**e**) Northern blot of Ago1-associated RNAs demonstrating that the tRNA-Glu sRNA (indicated with an asterisk) was specifically detected from *cid14Δ* cells, but not from wild-type cells, in a *dcr1*- and *rdp1*-independent manner. (**f**) Larger tRNA fragments are background contaminating RNAs, because they were also recovered from an untagged Ago1 strain. (**g**) ChIP experiment showing that H3K9me2 around the tRNA-Glu genes found in centromere 1 is not different in wild-type and *cid14Δ* cells. DNA from ChIP reactions with or without an antibody against H3K9me2 was used for PCR with primers to amplify *imr* fragments 1–5.

biogenesis and genomic distribution. Furthermore, our analysis of sRNAs in wild-type and *cid14Δ* cells revealed a previously unsuspected role for the RNA surveillance pathway involving the TRAMP complex in regulation of genomic siRNA distribution through removing entire classes of RNAs that have the potential to enter the sRNA pathways.

siRNA generation in fission yeast[13,17,18,47,48]. The requirement for Clr4 in both H3K9 methylation and siRNA generation has been suggested to indicate a chromatin-dependent step in recruitment of RITS and RDRC to their target transcripts[17,49]. Here we found detectable levels of antisense rr-siRNAs in Ago1 pull-downs from *clr4Δ* cells (**Fig. 5c**). These observations suggest that rRNAs can become targets for the RNAi machinery when the components of the RNAi pathway are released from centromeres as a result of the lack of H3K9 methylation in *clr4Δ* cells, thus allowing them to access rRNAs that would usually be processed by the TRAMP pathway. Furthermore, the high rRNA abundance is likely to overcome the requirement for H3K9 methylation–dependent recruitment of RDRC, allowing siRNA generation on rRNA substrates.

DISCUSSION
Our results provide a more comprehensive picture of Ago1-associated small RNAs in fission yeast and reveal new insights into their

Specific siRNA features
The vast majority of Ago1-associated sRNAs contained U at the 5′ position. This preference for 5′ U was mostly attributed to much higher stability of the 5′ U siRNAs, which reflects a marked loading preference for those siRNAs beginning with U. Although the relationship between 5′ nucleotide composition and biogenesis, loading and stability have not been teased apart in most other systems, this preference for a 5′ U in loading might be conserved in a large subset of Argonaute and Piwi family proteins. U is the preferred 5′ nucleotide of miRNAs of animals and plants[31,32], piRNAs of flies[33] and mammals[34–38] and 21U-RNAs of worms[30], although G is the preferred 5′ nucleotide of endogenous siRNAs of worms[29] and A is the preferred 5′ nucleotide of the most populated class of endogenous siRNAs in plants[28].
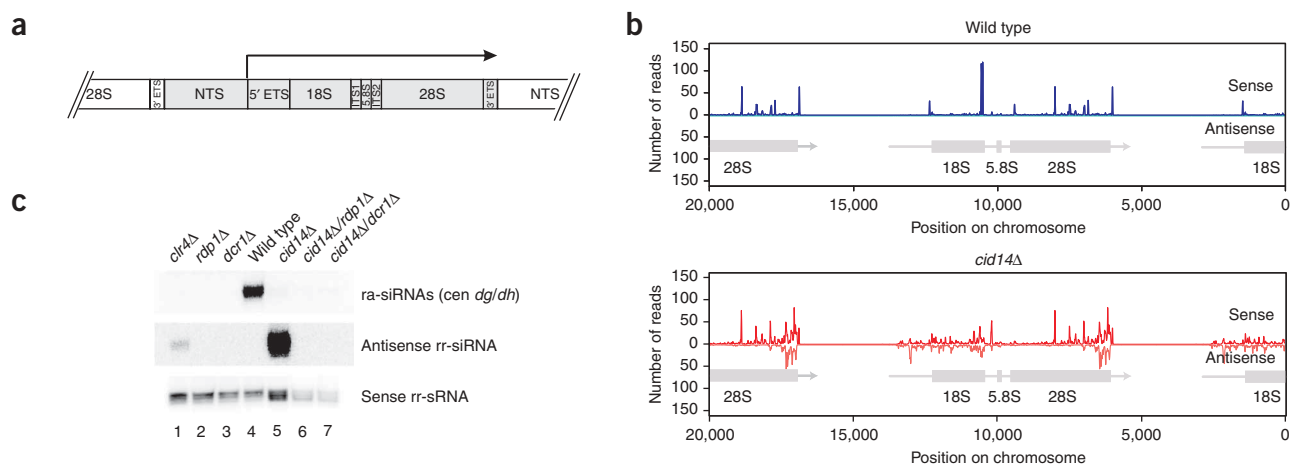
Figure 5 Ribosomal RNAs give rise to antisense siRNAs (rr-siRNAs) in *cid14Δ* cells. (**a**) Structure of the *S. pombe* rDNA unit[45]. The long precursor RNA indicated by the arrow is rapidly processed to form the mature 18S, 5.8S and 28S rRNAs through removal of the 5′ and 3′ external transcribed spacers (ETS) and the internal transcribed spacers (ITS) 1 and 2. The nontranscribed spacer (NTS) separates the different rRNA units at the rDNA locus. (**b**) Antisense rr-siRNAs are produced only in *cid14Δ* cells. Antisense rr-siRNAs are more or less equally distributed along the 18S and 5.8S rRNAs, whereas most of the antisense 28S rr-siRNAs map to the 3′ end. (**c**) Antisense rr-siRNA biogenesis strictly depends on Rdp1 and Dcr1, but not Clr4. Northern blot was performed with Ago1-associated RNAs isolated from different genetic backgrounds as indicated. The same blot was consecutively hybridized with probes specific for either centromeric *dg/dh* repeat–associated siRNAs (ra-siRNAs), antisense rr-siRNAs or sense rr-sRNAs.

Role of Cid14 in regulation of siRNA distribution

Members of the family of noncanonical poly(A) polymerases that includes Cid14 seem to have central roles in surveillance mechanisms that monitor RNA quality. These enzymes are involved in rRNA processing, tRNA processing, snoRNA processing and the interferon response[23,50]. Furthermore, members of this family have been implicated in RNAi and siRNA biogenesis in *C. elegans*, *S. pombe* and *Tetrahymena thermophila*[17,20,51,52]. They are therefore likely to have a broad and ancient role in coordination of endogenous RNA quality control and the recognition of aberrant and foreign RNAs.

In addition to Cid14, another member of the fission yeast family of noncanonical poly(A) polymerases, Cid12, has previously been implicated in siRNA biogenesis[17]. Whereas in cells lacking Cid12 cen siRNAs are absent[17], cen siRNA levels in *cid14Δ* cells are dramatically reduced[20]. Our results provide an explanation for this

reduction in cen siRNA levels. Cid14 is a subunit of the TRAMP polyadenylation complex, which is involved in recognition and targeting of aberrant RNAs for exosomal degradation[22,25]. Recognition is thought to involve polyadenylation of aberrant 3′ ends by Trf4 in *S. cerevisiae* and Cid14 in *S. pombe*. Notably, Cid12 is a stable component of the RDRC complex, which is required for RNAi-mediated heterochromatin formation[17]. Together with our present observations on the specific appearance of antisense rRNA siRNAs (rr-siRNAs) in *cid14Δ* cells, these results suggest a model for the regulation of siRNA levels from different genomic regions that involves competition between the TRAMP and RDRC complexes for RNA substrates, mediated by the
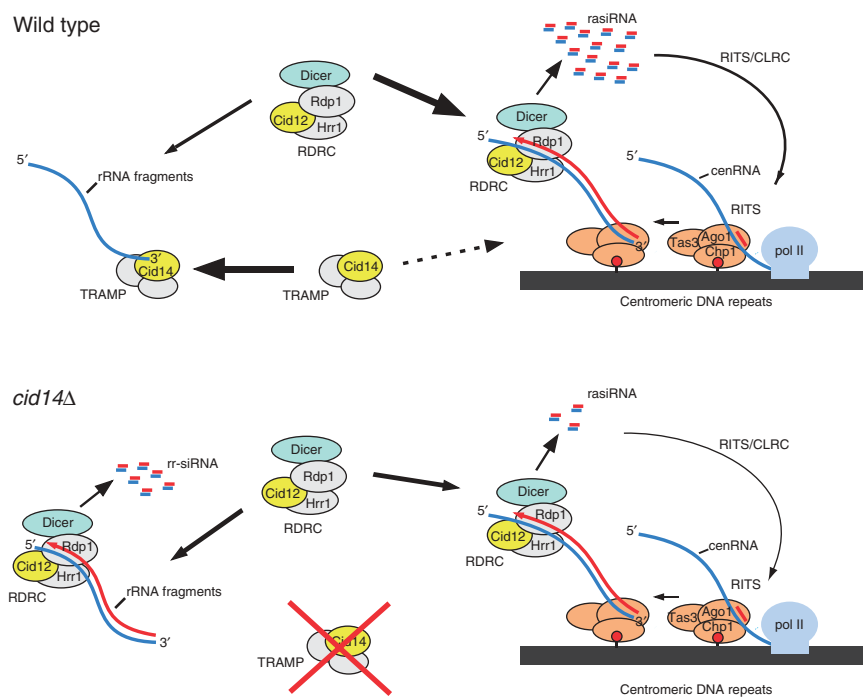
Figure 6 Model for competition between the RNAi and the Cid14–TRAMP RNA surveillance pathways. In wild-type cells, RDRC and Dicer are recruited to centromeric repeats by the RITS complex, which is tethered to chromatin via siRNA-dependent base-pairing interactions with noncoding centromeric RNA (cenRNA) and association with H3K9 methylated nucleosomes (red lollipops). This results in dsRNA synthesis and the generation of repeat-associated siRNAs (rasiRNAs), which mediate further RITS recruitment coupled to H3K9 methylation by the Clr4-containing CLRC methyltransferase complex. The TRAMP complex targets rRNA fragments for exosomal degradation. In *cid14Δ* cells, rRNA fragments accumulate and become substrates for RDRC and Dicer. This titrates RDRC and Dicer away from cenRNA, resulting in the generation of rRNA-siRNAs (rr-siRNAs) and a reduction in rasiRNAs.

two poly(A) polymerase proteins Cid12 and Cid14. In this model, Cid12 and Cid14 would have preferences for different substrates but could also act on noncanonical substrates. For example, Cid14 would normally promote the targeting of rRNA precursors or the tRNA-Glu fragment for exosomal degradation or processing. In the absence of Cid14, such precursors accumulate and become targets for RDRC, recruit RDRC away from centromeric transcripts, and thus give rise to rr-siRNAs with a concomitant decrease in cen siRNAs (**Fig. 6**). In support of this competition model, we also observe the emergence of antisense rr-siRNAs in *clr4Δ* cells. Clr4 is required for efficient cen siRNA generation and for the physical association of RDRC with RITS and centromeric transcripts, and localization of RDRC to centromeric DNA repeats[17]. The release of RDRC (Cid12) from heterochromatic regions probably allows RDRC to more effectively compete for abundant rRNA precursors, even in the presence of a functional TRAMP complex.

A second possible level of competition could arise from the preference of Ago1 for small RNAs with a 5′ U, independently of RDRC and Dcr1. In this case, any small RNA with a 5′ U not degraded by TRAMP and exosome would have the potential to load onto and therefore sequester Ago1. Presumably, those sRNAs that resemble Dcr1 products in being double stranded with 2-nt 3′ overhangs would have the benefit of preferential loading into Ago1, but even single-stranded sRNAs would have some ability to be loaded into, or at least associated with, Ago1. As a result, aberrant RNAs may directly interfere with Ago1 function at centromeres, providing another possible explanation for reduced cen siRNA levels in *cid14Δ* cells. In support of this model, we find that Ago1 is associated with massive amounts of an sRNA, starting with 5′ U and matching sense to tRNA-Glu, in *cid14Δ* cells. Although this sRNA may not be functional, its sheer abundance in ago1-associated small RNAs (14% of total reads) suggests that it may directly interfere with Ago1 function at centromeres, contributing to the reduced cen siRNA levels in *cid14Δ* cells.

Gene-specific sRNAs

A substantial portion (~28,000, 13%) of the Ago1-associated sRNAs in this study map to genes and intergenic regions (**Figs. 1** and **3**, and **Supplementary Table 3**). In particular, we note that the sRNAs that map to intergenic regions account for a large fraction (~22%) of this class. Although intergenic regions are not expected to be as highly transcribed as annotated genes, they are transcribed to some extent. A recent study suggests that extensive read-through transcription occurs at convergent gene pairs in the G1 phase of the cell cycle, giving rise to overlapping sense and antisense transcripts[53]. Such overlapping transcripts are proposed to create a dsRNA substrate for siRNA generation by Dicer, which then leads to RITS recruitment and transient heterochromatin formation[53]. However, Ago1-bound sRNAs do not preferentially correspond to convergent gene pairs, suggesting that siRNAs resulting from overlapping transcripts in these regions may be too rare in asynchronous fission yeast cultures to be represented above the level of background Ago1-bound gene-specific sRNAs. Finally, we note that global analyses of H3K9 methylation and RNA levels show that, for most *S. pombe* genes, neither H3K9 methylation nor RNA levels change substantially in RNAi mutants[16,54]. These observations suggest that the sRNAs identified in our study may act at the post-transcriptional level, but the functional relevance of the gene-specific sRNAs, if any, remains speculative and requires further investigation.

In conclusion, eukaryotes have evolved elaborate surveillance mechanisms to monitor the quality of the transcriptome. These mechanisms often involve the degradation of aberrant RNAs that lack proper processing signals. Translation-dependent mechanisms such as nonsense-mediated mRNA decay act in the cytoplasm to control the quality of open reading frames and thereby prevent the production of potentially malfunctioning proteins. The surveillance system also recognizes and degrades other types of aberrant transcripts, some of which lack the potential to be translated into protein. As we show in this study, such aberrant RNAs may have deleterious effects by interfering with the generation of endogenous siRNAs or serving as templates to generate new siRNAs with the potential to silence genetic information.

METHODS

Fission yeast strains and plasmids. The plasmid pREP1-3×Flag-Ago1 was described previously[14]. *Schizosaccharomyces pombe* strains used in this study are described in **Supplementary Table 4** online and were grown at 30 °C in YEA medium (yeast extract supplemented with adenine). If transformed with pREP1-3×Flag-Ago1, cells were grown at 30 °C in EMMC–leu+his medium.

Generation of small RNA libraries for 454 deep sequencing. Ago1-associated RNA was isolated as described previously[20] and 20–30-nt RNAs were PAGE purified. The eluted small RNAs were cloned based upon the preactivated, adenylated linkering method described previously[31] using a mutant T4 RNA ligase (Rnl2$_{1–249}$)[55]. Single-stranded DNA suitable to go directly into the emulsion PCR step of 454 pyrosequencing was generated as described previously[27].

In silico analysis of sequencing data. We selected 454 reads with matches to the terminal 9 nt of the 5′ linker and the first 9 nt of the 3′ linker, which resulted in a total of 349,477 wild-type reads and 315,701 reads in *cid14Δ*. Next, we mapped reads of size 15–29 nt to the *S. pombe* genome, requiring a perfect match to the genome. This yielded 255,487 reads (73%) in wild-type and 240,471 reads (76%) in *cid14Δ*, which we analyzed in this paper. We used the genome and annotations that were current as of 18 July 2007, available from The *S. pombe* Genome Project (http://www.sanger.ac.uk/Projects/S_pombe/). Unless otherwise noted, all read counts were normalized by the number of times the read perfectly matched the genome. The mating-type K-region was obtained from PubMed (U57841).

DNA oligonucleotides. Sequences of the DNA oligonucleotides used in this study are described in **Supplementary Table 5** online.

Northern blot analysis. Ago1-associated RNAs were recovered from Flag-purified Flag-Ago1 protein and analyzed by northern blot as described previously[20]. To detect centromeric siRNAs (cen *dg/dh*), a mixture of oligonucleotides complementary to the siRNAs sequenced by Reinhart and Bartel[15] were 5′ end labeled. Sense ribosomal small RNAs (rsRNAs), antisense ribosomal siRNAs (rsiRNAs) and tRNA-Glu sRNAs were detected with labeled DNA oligonucleotides rsi1-10, rsi11-18 and mb512, respectively.

Chromatin immunoprecipitation. ChIP was performed with the antibody ab1220 (abcam) as described previously[18]. Primers to amplify IRC3R and actin were mb510/511 and mb90/91, respectively. Primers to amplify *dh*/imr1R sequences 1–5 surrounding the tRNA-Glu gene were DM566/567, mb527/528, mb521/522, mb523/524 and mb525/526, respectively.

Accession codes. Gene Expression Omnibus: small RNA sequencing data were deposited with the accession number GSE12416.

Note: Supplementary information is available on the Nature Structural & Molecular Biology website.

1. Fire, A. *et al.* Potent and specific genetic interference by double-stranded RNA in *Caenorhabditis elegans. Nature* **391**, 806–811 (1998).
2. Hannon, G.J. RNA interference. *Nature* **418**, 244–251 (2002).
3. Hamilton, A.J. & Baulcombe, D.C. A species of small antisense RNA in posttranscriptional gene silencing in plants. *Science* **286**, 950–952 (1999).
4. Hammond, S.M., Bernstein, E., Beach, D. & Hannon, G.J. An RNA-directed nuclease mediates post-transcriptional gene silencing in *Drosophila* cells. *Nature* **404**, 293–296 (2000).
5. Zamore, P.D., Tuschl, T., Sharp, P.A. & Bartel, D.P. RNAi: double-stranded RNA directs the ATP-dependent cleavage of mRNA at 21 to 23 nucleotide intervals. *Cell* **101**, 25–33 (2000).
6. Elbashir, S.M., Lendeckel, W. & Tuschl, T. RNA interference is mediated by 21- and 22-nucleotide RNAs. *Genes Dev.* **15**, 188–200 (2001).
7. Bernstein, E., Caudy, A.A., Hammond, S.M. & Hannon, G.J. Role for a bidentate ribonuclease in the initiation step of RNA interference. *Nature* **409**, 363–366 (2001).
8. Baulcombe, D. RNA silencing in plants. *Nature* **431**, 356–363 (2004).
9. Sijen, T. *et al.* On the role of RNA amplification in dsRNA-triggered gene silencing. *Cell* **107**, 465–476 (2001).
10. Zaratiegui, M., Irvine, D.V. & Martienssen, R.A. Noncoding RNAs and gene silencing. *Cell* **128**, 763–776 (2007).
11. Buhler, M. & Moazed, D. Transcription and RNAi in heterochromatic gene silencing. *Nat. Struct. Mol. Biol.* **14**, 1041–1048 (2007).
12. Volpe, T.A. *et al.* Regulation of heterochromatic silencing and histone H3 lysine-9 methylation by RNAi. *Science* **297**, 1833–1837 (2002).
13. Verdel, A. *et al.* RNAi-mediated targeting of heterochromatin by the RITS complex. *Science* **303**, 672–676 (2004).
14. Buker, S.M. *et al.* Two different Argonaute complexes are required for siRNA generation and heterochromatin assembly in fission yeast. *Nat. Struct. Mol. Biol.* **14**, 200–207 (2007).
15. Reinhart, B.J. & Bartel, D.P. Small RNAs correspond to centromere heterochromatic repeats. *Science* **297**, 1831 (2002).
16. Cam, H.P. *et al.* Comprehensive analysis of heterochromatin- and RNAi-mediated epigenetic control of the fission yeast genome. *Nat. Genet.* **37**, 809–819 (2005).
17. Motamedi, M.R. *et al.* Two RNAi complexes, RITS and RDRC, physically interact and localize to noncoding centromeric RNAs. *Cell* **119**, 789–802 (2004).
18. Buhler, M., Verdel, A. & Moazed, D. Tethering RITS to a nascent transcript initiates RNAi- and heterochromatin-dependent gene silencing. *Cell* **125**, 873–886 (2006).
19. Sadaie, M., Iida, T., Urano, T. & Nakayama, J. A chromodomain protein, Chp1, is required for the establishment of heterochromatin in fission yeast. *EMBO J.* **23**, 3825–3835 (2004).
20. Buhler, M., Haas, W., Gygi, S.P. & Moazed, D. RNAi-dependent and -independent RNA turnover mechanisms contribute to heterochromatic gene silencing. *Cell* **129**, 707–721 (2007).
21. Chen, E.S. *et al.* Cell cycle control of centromeric repeat transcription and heterochromatin assembly. *Nature* **451**, 734–737 (2008).
22. LaCava, J. *et al.* RNA degradation by the exosome is promoted by a nuclear polyadenylation complex. *Cell* **121**, 713–724 (2005).
23. Stevenson, A.L. & Norbury, C.J. The Cid1 family of non-canonical poly(A) polymerases. *Yeast* **23**, 991–1000 (2006).
24. Win, T.Z. *et al.* Requirement of fission yeast Cid14 in polyadenylation of rRNAs. *Mol. Cell. Biol.* **26**, 1710–1721 (2006).
25. Vanacova, S. *et al.* A new yeast poly(A) polymerase complex involved in RNA quality control. *PLoS Biol.* **3**, e189 (2005).
26. Wyers, F. *et al.* Cryptic Pol II transcripts are degraded by a nuclear quality control pathway involving a new poly(A) polymerase. *Cell* **121**, 725–737 (2005).
27. Margulies, M. *et al.* Genome sequencing in microfabricated high-density picolitre reactors. *Nature* **437**, 376–380 (2005).
28. Rajagopalan, R., Vaucheret, H., Trejo, J. & Bartel, D.P. A diverse and evolutionarily fluid set of microRNAs in *Arabidopsis thaliana. Genes Dev.* **20**, 3407–3425 (2006).
29. Ambros, V., Lee, R.C., Lavanway, A., Williams, P.T. & Jewell, D. MicroRNAs and other tiny endogenous RNAs in *C. elegans. Curr. Biol.* **13**, 807–818 (2003).
30. Ruby, J.G. *et al.* Large-scale sequencing reveals 21U-RNAs and additional microRNAs and endogenous siRNAs in *C. elegans. Cell* **127**, 1193–1207 (2006).
31. Lau, N.C., Lim, L.P., Weinstein, E.G. & Bartel, D.P. An abundant class of tiny RNAs with probable regulatory roles in *Caenorhabditis elegans. Science* **294**, 858–862 (2001).
32. Reinhart, B.J., Weinstein, E.G., Rhoades, M.W., Bartel, B. & Bartel, D.P. MicroRNAs in plants. *Genes Dev.* **16**, 1616–1626 (2002).
33. Aravin, A.A. *et al.* The small RNA profile during *Drosophila melanogaster* development. *Dev. Cell* **5**, 337–350 (2003).
34. Aravin, A. *et al.* A novel class of small RNAs bind to MILI protein in mouse testes. *Nature* **442**, 203–207 (2006).
35. Lau, N.C. *et al.* Characterization of the piRNA complex from rat testes. *Science* **313**, 363–367 (2006).
36. Girard, A., Sachidanandam, R., Hannon, G.J. & Carmell, M.A. A germline-specific class of small RNAs binds mammalian Piwi proteins. *Nature* **442**, 199–202 (2006).
37. Grivna, S.T., Beyret, E., Wang, Z. & Lin, H. A novel class of small RNAs in mouse spermatogenic cells. *Genes Dev.* **20**, 1709–1714 (2006).
38. Watanabe, T. *et al.* Identification and characterization of two novel classes of small RNAs in the mouse germline: retrotransposon-derived siRNAs in oocytes and germline small RNAs in testes. *Genes Dev.* **20**, 1732–1743 (2006).
39. Rand, T.A., Petersen, S., Du, F. & Wang, X. Argonaute2 cleaves the anti-guide strand of siRNA during RISC activation. *Cell* **123**, 621–629 (2005).
40. Matranga, C., Tomari, Y., Shin, C., Bartel, D.P. & Zamore, P.D. Passenger-strand cleavage facilitates assembly of siRNA into Ago2-containing RNAi enzyme complexes. *Cell* **123**, 607–620 (2005).
41. Irvine, D.V. *et al.* Argonaute slicing is required for heterochromatic silencing and spreading. *Science* **313**, 1134–1137 (2006).
42. Schwarz, D.S. *et al.* Asymmetry in the assembly of the RNAi enzyme complex. *Cell* **115**, 199–208 (2003).
43. Allshire, R.C., Javerzat, J.P., Redhead, N.J. & Cranston, G. Position effect variegation at fission yeast centromeres. *Cell* **76**, 157–169 (1994).
44. Scott, K.C., Merrett, S.L. & Willard, H.F. A heterochromatin barrier partitions the fission yeast centromere into discrete chromatin domains. *Curr. Biol.* **16**, 119–129 (2006).
45. Good, L., Intine, R.V. & Nazar, R.N. The ribosomal-RNA-processing pathway in *Schizosaccharomyces pombe. Eur. J. Biochem.* **247**, 314–321 (1997).
46. Wang, S.W., Stevenson, A.L., Kearsey, S.E., Watt, S. & Bahler, J. Global role for polyadenylation-assisted nuclear RNA degradation in posttranscriptional gene silencing. *Mol. Cell. Biol.* **28**, 656–665 (2008).
47. Hong, E.J., Villen, J., Gerace, E.L., Gygi, S.P. & Moazed, D. A cullin E3 ubiquitin ligase complex associates with Rik1 and the Clr4 histone H3–K9 methyltransferase and is required for RNAi-mediated heterochromatin formation. *RNA Biol.* **2**, 106–111 (2005).
48. Li, F. *et al.* Two novel proteins, Dos1 and Dos2, interact with Rik1 to regulate heterochromatic RNA interference and histone modification. *Curr. Biol.* **15**, 1448–1457 (2005).
49. Verdel, A. & Moazed, D. RNAi-directed assembly of heterochromatin in fission yeast. *FEBS Lett.* **579**, 5872–5878 (2005).
50. Justesen, J., Hartmann, R. & Kjeldgaard, N.O. Gene structure and function of the 2′-5′-oligoadenylate synthetase family. *Cell. Mol. Life Sci.* **57**, 1593–1612 (2000).
51. Chen, C.C. *et al.* A member of the polymerase β nucleotidyltransferase superfamily is required for RNA interference in *C. elegans. Curr. Biol.* **15**, 378–383 (2005).
52. Lee, S.R. & Collins, K. Physical and functional coupling of RNA-dependent RNA polymerase and Dicer in the biogenesis of endogenous siRNAs. *Nat. Struct. Mol. Biol.* **14**, 604–610 (2007).
53. Gullerova, M. & Proudfoot, N.J. Cohesin complex promotes transcriptional termination between convergent genes in *S. pombe. Cell* **132**, 983–995 (2008).
54. Hansen, K.R. *et al.* Global effects on gene expression in fission yeast by silencing and RNA interference machineries. *Mol. Cell. Biol.* **25**, 590–601 (2005).
55. Ho, C.K., Wang, L.K., Lima, C.D. & Shuman, S. Structure and mechanism of RNA ligase. *Structure* **12**, 327–339 (2004).